

## Characterization of heterogeneity in the molecular pathogenesis of lupus nephritis from transcriptional profiles of laser-captured glomeruli

Karin S. Peterson, ... , Michael R. Jackson, Robert J. Winchester

*J Clin Invest.* 2004;113(12):1722-1733. <https://doi.org/10.1172/JCI19139>.

Article Autoimmunity

The molecular pathogenesis of focal/diffuse proliferative lupus glomerulonephritis was studied by cDNA microarray analysis of gene expression in glomeruli from clinical biopsies. Transcriptional phenotyping of glomeruli isolated by laser-capture microscopy revealed considerable kidney-to-kidney heterogeneity in increased transcript expression, resulting in four main gene clusters that identified the presence of B cells, several myelomonocytic lineages, fibroblast and epithelial cell proliferation, matrix alterations, and expression of type I IFN-inducible genes. Glomerulus-to-glomerulus variation within a kidney was less marked. The myeloid lineage transcripts, characteristic of those found in isolated activated macrophages and myeloid dendritic cells, were widely distributed in all biopsy samples. One major subgroup of the samples expressed fibrosis-related genes that correlated with pathological evidence of glomerulosclerosis; however, decreased expression of TGF- $\beta$ 1 argued against its role in lupus renal fibrosis. Expression of type I IFN-inducible transcripts by a second subset of samples was associated with reduced expression of fibrosis-related genes and milder pathological features. This pattern of gene expression resembled that exhibited by activated NK cells. A large gene cluster with decreased expression found in all samples included ion channels and transcription factors, indicating a loss-of-function response to the glomerular injury.

Find the latest version:

<https://jci.me/19139/pdf>





# Characterization of heterogeneity in the molecular pathogenesis of lupus nephritis from transcriptional profiles of laser-captured glomeruli

Karin S. Peterson,<sup>1</sup> Jing-Feng Huang,<sup>2</sup> Jessica Zhu,<sup>2</sup> Vivette D'Agati,<sup>3</sup> Xuejun Liu,<sup>2</sup> Nancy Miller,<sup>4</sup> Mark G. Erlander,<sup>2</sup> Michael R. Jackson,<sup>2</sup> and Robert J. Winchester<sup>1,3</sup>

<sup>1</sup>Department of Pediatrics, Columbia University, New York, New York, USA. <sup>2</sup>Johnson & Johnson Pharmaceutical Research and Development, San Diego, California, USA. <sup>3</sup>Department of Pathology, Columbia University, New York, New York, USA. <sup>4</sup>Omniviz Inc., Maynard, Massachusetts, USA.

**The molecular pathogenesis of focal/diffuse proliferative lupus glomerulonephritis was studied by cDNA microarray analysis of gene expression in glomeruli from clinical biopsies. Transcriptional phenotyping of glomeruli isolated by laser-capture microscopy revealed considerable kidney-to-kidney heterogeneity in increased transcript expression, resulting in four main gene clusters that identified the presence of B cells, several myelomonocytic lineages, fibroblast and epithelial cell proliferation, matrix alterations, and expression of type I IFN-inducible genes. Glomerulus-to-glomerulus variation within a kidney was less marked. The myeloid lineage transcripts, characteristic of those found in isolated activated macrophages and myeloid dendritic cells, were widely distributed in all biopsy samples. One major subgroup of the samples expressed fibrosis-related genes that correlated with pathological evidence of glomerulosclerosis; however, decreased expression of TGF- $\beta$ 1 argued against its role in lupus renal fibrosis. Expression of type I IFN-inducible transcripts by a second subset of samples was associated with reduced expression of fibrosis-related genes and milder pathological features. This pattern of gene expression resembled that exhibited by activated NK cells. A large gene cluster with decreased expression found in all samples included ion channels and transcription factors, indicating a loss-of-function response to the glomerular injury.**

## Introduction

Systemic lupus erythematosus (SLE) is a genetically determined autoimmune disease in which a T cell-driven adaptive immune response results in the formation of autoantibodies, most notably directed against DNA, RNA, and their associated proteins (1, 2). Classically, the resulting immune complexes have been considered to initiate renal disease, one of the most significant causes of morbidity and mortality in lupus, through complement activation in a neutrophil-mediated Arthus-type reaction. However, evidence from studies of spontaneous lupus in the New Zealand Black/White (NZB/W) mouse has indicated involvement of other pathways, including activation of myeloid cells via Fc receptor engagement, that are thought to mediate the inflammatory response (3).

The pathological manifestations of lupus nephritis are diverse, variably affecting the different renal compartments, including glomeruli, tubules, interstitium, and vasculature (4). Lupus glomerular injury takes several forms and is categorized into five classes: WHO classes I-V (4). A major feature of lupus nephritis is the considerable degree of variation in severity of histopathological involvement between different glomeruli from the same biopsy, and the histopathological classification is there-

fore based on the average score for all glomeruli in the biopsy. The most common and most severe forms, focal (class III) and diffuse (class IV) proliferative glomerulonephritis, share similar histopathological features and differ principally by the proportion and extent of glomerular involvement.

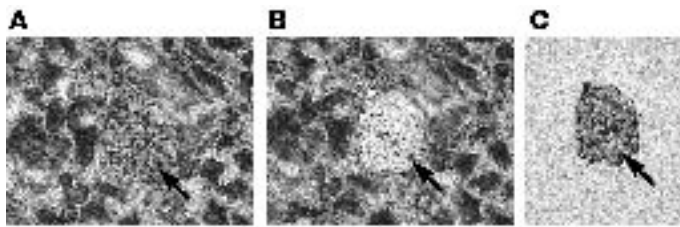
Importantly, the course, response to therapy, and outcome are heterogeneous among affected individuals, with nearly one in three progressing to glomerulosclerosis and end-stage renal disease, while the others either respond to therapy or follow a milder course (4). These differences in outcome are not well correlated with WHO class (4). Efforts at better predicting outcome and therapeutic requirements from biopsy morphology were initiated by Pollack et al., whose distinction of active and sclerosing lesions led to the development of the activity and chronicity indices (5, 6). Although there is a positive correlation of elevated chronicity index with progression to chronic renal insufficiency, the lack of a clear threshold value, low sensitivity, and problems in reproducibility have limited the utility of the morphological indices (7). These points raise the question of whether there are additional differences not identified at the level of conventional histopathology that are relevant to the nature of the renal injury and emphasize the need to analyze the pathogenesis of lupus nephritis at the molecular level.

The application of the microarray technique to the monitoring of gene expression profiles has provided significant insights into the biology of different neoplasms and has demonstrated its value in the approach to their subclassification (8). However, there are significant problems raised by the application of this methodology to lupus nephritis. First, the architecture of the kidney is complex and

**Nonstandard abbreviations used:** comparative threshold ( $C_T$ ); Fc receptor (FcR); New Zealand Black/White (NZB/W); quantitative real-time PCR (qRT-PCR); systemic lupus erythematosus (SLE).

**Conflict of interest:** The authors have declared that no conflict of interest exists.

**Citation for this article:** *J. Clin. Invest.* 113:1722–1733 (2004). doi:10.1172/JCI200419139.

**Figure 1**

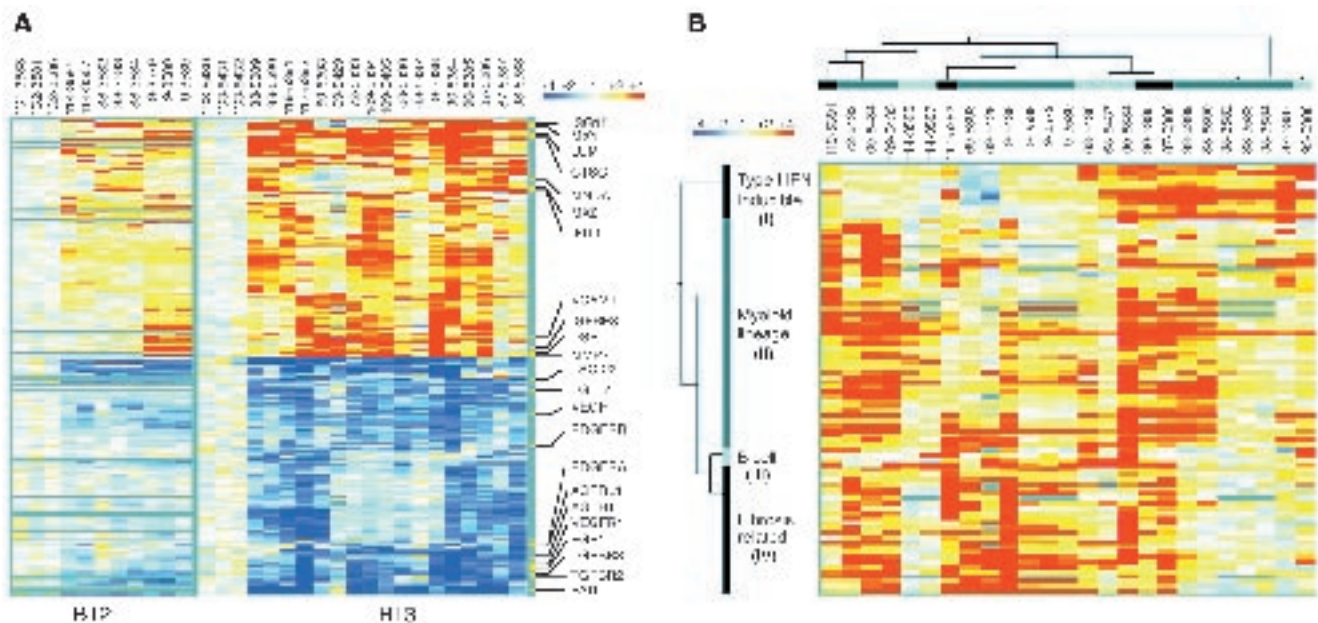
Laser-capture microdissection. (A–C) Isolation of a glomerulus by laser-capture microdissection from a hematoxylin and eosin–stained section of a lupus renal biopsy cut 7  $\mu\text{m}$  in thickness. The arrow in **A** shows a glomerulus prior to capture. Activation by laser of a heat-sensitive film, placed in direct contact with the tissue section, causes the cells located in the path of the laser to adhere to the film, and they can be lifted out of the tissue section. **C** indicates the successful film transfer of the captured glomerulus used for RNA extraction. **B** demonstrates the remaining biopsy after laser capture of the glomerulus. Magnification,  $\times 20$ .

different structural regions of the kidney exhibit distinctive gene expression profiles (9). Because lupus nephritis affects each compartment of the kidney in different ways, with the most profound primary immune complex injury at the level of the glomerulus, it is advantageous to study glomerular gene expression separately from that of the interstitium and tubules. Second, the potential for inflammation-related alterations in multiple renal cell lineages and

the presence of infiltrating inflammatory cells complicate the interpretation of the results. Finally, only the limited “archival material” remaining after diagnostic renal biopsy interpretation is available for research purposes, constraining the scope of potential studies. The technology described by Luo et al. (10) that integrates laser-capture microscopy of individual cells with linear RNA amplification and cDNA microarray analysis offers an approach for overcoming these limitations. This combined technology recently has been applied to the analysis of malignant and premalignant tissues (11–13). In the present study, we first sought to determine the feasibility of using laser-captured human glomeruli to examine the gene expression profiles of archival clinical lupus biopsies. In addition, we wished to determine whether microarray analysis could assist in the identification of molecular processes underlying lupus glomerular disease, with the ultimate goal of identifying molecular pathways and their heterogeneity that may be responsible for specific disease features and their relationship to the autoimmune process.

## Results

*Hierarchical clustering of genes differentially expressed in SLE glomeruli compared with controls.* Glomeruli were isolated successfully from the surrounding tissue by laser-capture microscopy, as documented by microscopic visualization of glomeruli before and after laser capture (Figure 1), and the transcriptional phenotypes of the glomeruli were determined using amplified RNA in microarray analyses. Compared

**Figure 2**

Gene expression profiles of lupus glomeruli. (A and B) Hierarchical clustering analysis of 25 lupus glomeruli, isolated from 12 different SLE biopsies, and 6 control glomeruli, isolated from 4 different control kidneys. Each row corresponds to a cDNA on the microarray and each column, to a glomerular sample. Along the tops of **A** and **B**, each lupus sample is identified by a number in which the part before the dash identifies the biopsy and the part after the dash identifies the individual glomerular sample. In **A**, controls (\*C) are shown and are identified by number as described above. The linear intensity scale ranges from fourfold or higher (+4) to minus fourfold or lower (–4). A positive “fold change” (yellow to red) indicates increased expression and a negative “fold change” (light to dark blue) indicates decreased expression in a glomerular sample compared with the average of the controls. **A** shows hierarchical clustering of 88 genes with increased expression and 89 genes with decreased expression in lupus glomeruli compared with the average of the controls, analyzed independently in sample set B12 and sample set B13. The location of some cDNA rows is indicated by their respective gene symbol along the right side of the clustering diagram. Supplemental Table 1 lists all genes that were clustered in **A**. **B** shows the combined hierarchical clustering of all genes with increased expression in lupus glomeruli in sample set B12 and B13. Four main gene clusters are shown (left margin) and are labeled as described in Results.



**Table 1**  
Immuno- and histopathology summary for each glomerulus studied

Biopsy identifier	109	72	9	117	69	68	90	114	119	93	87	38
Glomerular sample	5435 5434	5433 5438 3580 3579 3589	5438 3580 3579 3589	5392 5393 5429	5437 5436	5384 5385	3587 3585	5391 5391	5388 5388	5386 5387	5389 5390 3582 3583 3584	
<b>Immunopathology<sup>A</sup></b>												
T cells (CD3)	0	1	2	1	1	0	1	2	2	1	1	0
Monocytes (CD68)	2	3	3	3	1	1	3	3	3	2	2	2
<b>Markers of activity<sup>B</sup></b>												
Neutrophils	2	1	2	3	1	0	1	3	0	1	1	1
Endocapillary proliferation	2	2	3	3	1	1	3	3	3	3	2	2
Necrosis	0	1	1	1	1	0	1	3	1	2	3	1
Cellular crescents	2	0	3	3	0	0	1	1	1	1	1	0
Wire loops	2	1	2	2	0	0	3	0	1	1	1	1
Interstitial inflammation	1	2	2	2	1	3	3	1	0	1	1	0
Activity index	11	8	17	18	5	4	14	15	8	12	13	6
<b>Markers of chronicity<sup>B</sup></b>												
Glomerular sclerosis	1	2	1	1	1	1	2.5	1	1	0	0	1
Fibrous crescents	1	1	2	1	1	1	2	1	0	1	1	0
Tubular atrophy	0	2	1	0.5	0.5	1	2	0	0.5	0	0	0.5
Interstitial fibrosis	0	2	1	0.5	0.5	1	2	0	0.5	0	0	0.5
Chronicity index	2	7	5	3	3	4	8.5	2	2	1	1	2
<b>WHO class</b>	IV	IV	IV	IV	III	III	IV	IV	IV	IV	IV	IV

<sup>A</sup>The scale for quantification of infiltrating CD3- and CD68-positive cells was as follows: 0, no infiltrating cells; 1, up to one infiltrating cell per glomerulus; 2, two to five infiltrating cells per glomerulus; and 3, more than five infiltrating cells per glomerulus. <sup>B</sup>The scale for all markers of pathology (0–3) was averaged across all glomeruli in the formalin-fixed portion of the biopsy processed for routine light microscopy. The activity index (0–24) is the sum of the individual activity markers, with the score for crescents and necrosis accorded “double weight.” The chronicity index (0–12) is the sum of the individual chronicity markers.

with the mean value of expression in controls, SLE glomeruli exhibited one large cluster of genes with increased expression and one with decreased expression in each of two independent and separately processed and analyzed sets of lupus glomeruli studied on different cDNA microarrays (Figure 2A). Because of the high degree of similarity between the corresponding separate hierarchical clusters, the 88 genes with increased expression in the two data sets were merged and analyzed by hierarchical clustering (Figure 2B). Four main gene clusters with increased expression were identified (Supplemental Table 1; supplemental material available at <http://www.jci.org/cgi/content/full/113/12/1722/DC1>) and analyzed in detail (see below) for identification of their possible biological significance. Although the number of cDNAs on the microarray was limited and not inclusive of all possible genes in the clusters, we were able to discern biological characteristics likely related to function in each cluster. Briefly, seven of the eleven genes in cluster I were characterized by the presence of type I IFN response elements. Approximately half of the genes in cluster II contained transcripts that indicated the presence of cells of the myelomonocytic lineage in the glomerulus, and two of four genes in the small cluster III were expressed specifically in B cells. Cluster IV was characterized by the fact that more than one third of the transcripts were involved in the production or regulation of extracellular matrix (ECM), and this cluster appeared likely to be linked to the glomerulosclerosis (fibrosis) of lupus nephritis. Each transcript has been identified by its corresponding gene symbol as contained in LocusLink, which also includes the primary references to individual genes (14).

The large cluster of genes with decreased expression in lupus glomeruli, compared with that of controls, was in general uniformly decreased across all samples (Figure 2A). The transcripts included transcription factors and ion channels or were involved in aspects of cellular growth and differentiation (Supplemental Table 1). Some genes encoded molecules whose function in the kidney is not established. Unexpectedly, given their increased expression in some forms of glomerulosclerosis other than lupus (15, 16), both TGF-B1 (TGF-β1) and two of its receptor molecules, TGF-BR2 and TGF-BR3, exhibited significantly decreased expression in SLE glomeruli compared with controls, as did plasminogen activator inhibitor type 1 (PAI-1 or SERPINE; Figure 2A). Of note also was the decreased expression of transcripts involved in endothelial proliferation and angiogenesis, including VEGF, VEGFR1 (Flt1), and FGF1, particularly as endocapillary proliferation is a morphologic characteristic of class III/IV lupus nephritis (Table 1).



**Table 2**  
Clinical data for SLE patients studied by renal biopsy

Patient characteristics		119	72	109	114	117	69	9	68	90	87	38	93
Biopsy identifier													
Age/sex		27 yr/F	22 yr/F	22 yr/F	18 yr/F	38 yr/F	27 yr/F	28 yr/F	32 yr/F	45 yr/F	33 yr/F	28 yr/M	10 yr/M
Ethnicity		A	B	H	B	B	C	H	A	A	H	A	H
Diagnosis of SLE (mo) <sup>A</sup>		11	72	48	<1 <sup>F</sup>	<1	6	48	24	2	<1	156	6
Diagnosis nephritis (mo) <sup>A</sup>		1	24	<1	<1	<1	1	<1	<1	1	<1	24	<1
Major extrarenal manifestations of SLE		Arthritis, alopecia, DLE	Interstitial pneumonitis	Rash, ITP	Arthritis	None	Arthritis, rash	None	Arthritis	Rash, serositis	Pancytopenia	Arthritis, rash, alopecia	None
WHO nephritis class		IV	IV	IV	IV	IV	III	IV	III	IV	IV	IV	IV
Glom. IgG deposition <sup>B</sup>		1+	3+	3+	2+	2–3+	2+	3+	3+	3+	3+	3+	3+
Glom. IgM deposition <sup>B</sup>		0	1+	2+	1+	1+	0	0	1+	1+	2+	2+	1+
Glom. C1/C3 deposition <sup>B</sup>		–/1+	2+/3+	3+/3+	1+/2+	1+/3+	–/1–2+	2+/3+	2+/3+	3+/2+	1+/2+	2+/3+	2+/3+
Anti-DNA (<35) <sup>C</sup>		92	82	62		19	21	113	39	35	>300		58
Complement <sup>D</sup>		Low	NI	Low	Low	Low	NI	Low	Low	Low	Low	Low	NI
Hemoglobin (g/l) (12–16)		11.1	13.1	12.7		8.7	13.5	9.5	11.3	7.9	7.4	13.7	10.1
Serum Cr mg/dl (<0.9)		1.2	1.8	1.2		2.2	0.6	1.8	0.8	11	0.5	1.1	0.5
Urinalysis <sup>E</sup>		3+	8.6	5	0.96	4+	4+	5.9	4+	3.3	5.5	>2.0	2.0
Medications prior to biopsy		Plaq, Cyt ×1	Pred,	Pred	Plaq	None	Pred, Cyt ×1	Pred,	None	None	None	Pred, Plaq, Aza	None

<sup>A</sup>Measured in months (mo) prior to the date of the renal biopsy. <sup>B</sup>Presence of IgG and IgM heavy chains and complement components C1 and C3, as determined by immunofluorescence staining of all biopsies (scale, 0–3+). <sup>C</sup>All laboratory values were obtained at time of renal biopsy. Normal values are given in parenthesis for anti-DNA, hemoglobin, and serum creatinine. <sup>D</sup>Analyzed by measurement of CH50 and/or C3 and C4. <sup>E</sup>The 24-hour urine proteins in grams are given when available; if not, the qualitative urinalysis by dipstick is listed (scale, 1+ to 4+). <sup>F</sup>Discoid lupus erythematosus (DLE) was diagnosed 60 months prior to the onset of SLE. H, Hispanic; B, black; C, Caucasian; A, Asian; Glom., glomerular; Cr, creatinine; Pred, Prednisone; Plaq, plaquenil; Cyt, cyclophosphamide; ×1, once; Aza, azathioprine; NI, normal; ITP, immune thrombocytopenia. Blank sections, information not available.

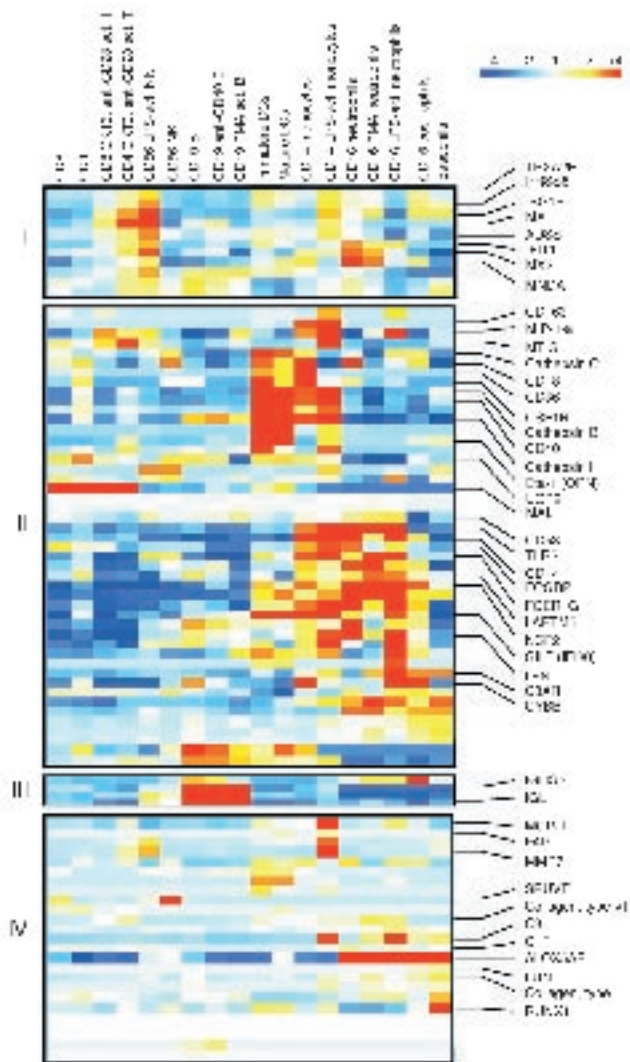
*Gene expression profiles of glomeruli isolated from the same biopsy cluster together.* As illustrated by the sample dendrogram in Figure 2B, different glomeruli obtained from the same patient biopsy were more concordant in their overall expression profiles than were glomeruli from different biopsies. Notably, in the case of biopsies 9 and 38, the gene expression profiles of glomeruli from the same biopsy clustered together even when analyzed in the independent data sets B12 and B13, despite some differences in expression intensity. The paired glomeruli from biopsies 69, 109, and 114 were also concordant in their overall gene expression. Conversely, the paired glomeruli from biopsies 68, 87, and 90 shared the expression of certain clusters but differed markedly in the expression of others, notably those of the fibrosis group.

*Increased expression of genes with type I IFN response elements.* Gene cluster I comprised 11 transcripts, most of which contained type I IFN response elements, and included G1P2 (ISG15), a ubiquitin-like molecule, and IFIT1, encoding the intracellular p56 protein, which inhibits protein synthesis. MX1 and MX2 are two large GTPases that belong to the dynamin family of microtubule-binding proteins; their specific function in man is not known in detail. MNDA (myeloid cell nuclear differentiation antigen) encodes a nuclear protein that promotes differentiation of the myeloid lineage, and SP100, a nuclear autoantigen and transcriptional enhancer. KIAA1268 exhibits significant DNA sequence homol-

ogy to an IFN- $\alpha$ -induced gene identified in the rainbow trout (17). Only thromboxane A2 receptor (TBXA2R), adenylosuccinate synthase (ADSS), prostasin (PRSS8), and the NCK adaptor protein 1 (NCK1) in this cluster lack IFN response elements.

A cell reference panel was used in an effort to identify patterns of infiltrating cell lineages among the glomerular expression profiles. A number of resting and activated peripheral blood cell cultures had been analyzed by microarray, and their expression profiles were linked by their gene identities to those of the glomerular samples, as shown in Figure 3. The top part of Figure 3 illustrates the overlap in expression between the transcripts of cluster I and the peripheral blood reference panel and demonstrates a strong expression of all cluster I genes by LPS-activated NK cells (CD56), but not by unstimulated NK cells. Some of the transcripts with type I IFN response elements were also expressed at lower levels by activated CD4 cells and cells of the neutrophil lineage.

*Increased expression of genes related to myelomonocytic and other inflammatory cells.* Cluster II was the most widely distributed cluster expressed by SLE glomeruli. Myelomonocytic cell lineage marker genes characterized this cluster and included CD14, CD40 (TNFRSF5), CD18 (ITGB2), CD53, C3 receptor (C3AR1), Toll-like receptor 2 (TLR2), and two components of the microbicidal oxidase system, NCF2 and CYBB. The mitogen-induced chemokine MIP-1- $\alpha$  (CCL3), involved in the recruitment and



activation of various inflammatory cells, was a highly expressed chemokine, along with Eta-1 (osteopontin; SPP1), a cytokine that is involved in early activation by T cells.

Pathways involved in the cellular uptake of antigen and immune complexes were suggested by a set of transcripts including CD36, CD163, FCGBP, and FCER1G. CD36 is a thrombospondin receptor that also functions as a scavenger receptor (18), and CD163 is a putative scavenger receptor present on myeloid cells. FCGBP is a mucin-rich IgG Fc receptor (FcγR) and FCER1G (FcRγc) is the signaling γ-chain that is common to several of the Fc receptors (FcRs).

**Figure 4**

Differential gene expression between two major subgroups of lupus glomeruli. Shown is the hierarchical clustering of genes with statistically significant difference in expression between the two major subpopulations of lupus glomeruli, SG1 and SG2, identified in this study. Lupus glomerular samples are listed along the top (identified as in Figure 2), and each row identifies a gene, labeled with its gene symbol on the right side of the figure. The linear intensity scale is the same as described in Figure 2. The expression levels in control glomeruli of the key transcripts that define the SG1 and SG2 lupus subpopulations are illustrated as described in Figure 2A.

**Figure 3**

Overlapping gene expression profiles between a peripheral blood cell reference panel and lupus glomeruli. Shown is the hierarchical clustering of transcripts expressed by resting and activated cells (cells listed at top) obtained from the peripheral blood of normal donors. Only genes that were increased in expression in lupus glomeruli (Figure 2B) were selected for clustering from the expression profiles of the peripheral blood cell reference panel. Each row represents a gene, and some gene names are listed along the right side of the figure. The gene rows have been subdivided on the left side of the figure according to the four main gene clusters (I–IV) identified in Figure 2B and described in Results. The linear intensity scale is the same as described in Figure 2. act., activated.

Also increased in expression were LYN and HCK, encoding two Src family kinases that are activated upon FcγR stimulation (19). Several transcripts indicated activation of the lysosomal antigen presentation pathway, including the lysosomal enzymes legumain (LGMN), cathepsin B (CTSB), cathepsin H (CTSH) and IFI30. The last encodes an IFN-γ-induced lysosomal thiol reductase (GILT) whose expression is essential for antigen presentation by MHC class II molecules and normal immune function (20).

It is clear from the gene expression profiles that the myeloid-related transcripts vary in their expression across lupus glomeruli, although elements of cluster II were present in almost all samples (Figure 2B), suggesting a heterogeneous pattern of infiltrating myeloid cells of different lineages and activation states. Additional evidence for the potential presence of a diverse set of myeloid cells was obtained by analyses of the parallels in expression between known genes in cluster II and the cell reference panel (Figure 3, II). Expression profiles characteristic of activated and resting neutrophils, monocytes, and dendritic cells could be identified among lupus-associated glomerular transcripts. However, individual cell lineages could not be assigned with certainty, as only a few transcripts were specific for an individual cell type; for example, Eta-1, expressed by dendritic cells.

Few transcripts were specific for T cells, among them MAL, a marker of the differentiated T cell lineage, which clustered with the myeloid transcripts. Analysis of expression of the lupus-associated transcripts by the peripheral blood reference set also demonstrated a paucity of T cell profiles in glomeruli, and the

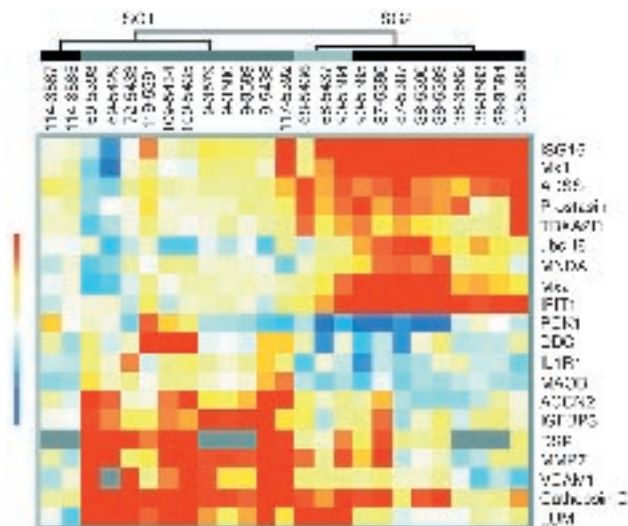




**Table 3**  
Correlation of molecular phenotype with histopathology

Gene expression phenotype Immunopathology	Type I IFN inducible			Fibrosis			B cell			Myeloid			Myeloid subcluster		
	Pos	P <sup>B</sup>	Neg	Pos	P	Neg	Pos	P	Neg	Pos	P	Neg	Pos	P	Neg
T cells (CD3)	0.6 <sup>A</sup>	0.017	1.4	1.1		0.6	1.2	0.004	0.3	1.1		0.5	1.1	0.062	0.4
Monocytes (CD68)	2.1		2.5	2.5		2	2.4		2.1	2.4		1.8	2.6	0.003	1.6
<b>Markers of activity</b>															
Neutrophils	0.9	0.002	1.9	1.5		1.2	1.5		1.1	1.5		1	1.6	0.056	0.9
Endocapillary proliferation	2.2		2.4	2.4		2.1	2.4	0.077	2	2.4		1.8	2.6	0.003	1.6
Necrosis	1.2		1.2	1		1.5	1.2		1.1	1.3		0.8	1.2		1.2
Cellular crescents	0.6	0.053	1.6	1.5	0.022	0.4	1.4	0.023	0.4	1.3	0.065	0.5	1.4	0.005	0.1
Wire loops	1.2		1.2	1.6	0.006	0.6	1.2		1.1	1.3		0.8	1.4	0.028	0.6
Interstitial inflammation	1.2		1.5	1.5		1	1.7	0.005	0.5	1.4		1	1.5		0.9
Activity index	9.3		11.6	12	0.027	7.7	11.5		7.8	11.3		7.3	11.8	0.012	6.4
<b>Markers of chronicity</b>															
Glomerular sclerosis	1		1.1	1.2		0.8	1.1		1	1.1		1	1.1		0.9
Fibrous crescents	0.7	0.023	1.4	1.3	0.021	0.6	1.3	0.002	0.4	1.1		0.7	1.2	0.059	0.6
Tubular atrophy	0.7		0.6	0.8		0.4	0.7		0.6	0.7		0.7	0.7		0.5
Interstitial fibrosis	0.7		0.6	0.8		0.4	0.7		0.6	0.7		0.7	0.7		0.5
Chronicity index	3.1		3.7	4.1	0.021	2.2	3.8		2.2	3.5		3	3.7		2.4

<sup>A</sup>Glomeruli were divided into two groups according to the presence (Pos, positive) or absence (Neg, negative) of gene expression phenotype, as illustrated in Figure 5. The mean score of each marker of pathology and immunopathology for the glomeruli in the respective group is recorded in the table. <sup>B</sup>Differences in markers of pathology and immunopathology between the two groups that express versus do not express a particular gene cluster were compared for statistical significance using the Wilcoxon rank sum test. P values less than 0.09 are listed.

activated CD4 cell was the only lineage that exhibited considerable overlap in gene expression (Figure 3).

The small but distinctive gene cluster III mainly reflected the presence of transcripts identifying immunoglobulin heavy (IGHG3) and light (IGL) chains and, as illustrated by Figure 3, this cluster was specifically expressed by B cells in the reference panel.

*Increased expression of genes related to ECM and glomerulosclerosis.* Gene cluster IV contained a set of transcripts known to be involved in the production or regulation of ECM that are likely to be involved in elements of the inflammatory response leading to lupus renal fibrosis and included lumican (LUM), collagen I and VI (COL1A2 and COL6A3), and matrilysin (MMP7). Epithelial proliferation and increased numbers of fibroblasts are additional features of fibrosis, and several transcripts in cluster IV indicated the presence of these two processes: desmoplakin (DSP) is involved in the formation of epithelial sheets and keratin 18 (KRT18) is an intermediate filament of simple epithelia. THY1 is a fibroblast marker and FAP is a fibroblast-activating protein not expressed by normal adult tissue but synthesized by reactive stromal fibroblasts in healing wounds.

Interestingly, this cluster also contains CCL2, encoding monocyte chemoattractant protein 1 (MCP-1), a chemokine previously linked to renal fibrosis (21). Other transcripts encode proteins that are related to inflammation and not known to be directly involved in the process of fibrosis, such as the arachidonate 5-lipoxygenase-activating protein (ALOX5AP), complement C3, C1r (C1R), and I factor (IF), and a hematopoietic transcription factor, RUNX1. Cathepsin C (CTSC) was highly and consistently present among these transcripts. Except for CCL2, which is expressed mainly by activated monocytes, and RUNX1, the fibrosis gene cluster contained few genes that were also expressed by cells in the blood reference panel (Figure 3, IV), suggesting that the majority of the cluster IV transcripts were derived from parenchymal cells. The source of MCP-1 (CCL2) is ambiguous, as the mesangial cell has been shown to synthesize this chemokine after exposure to inflammatory or mechanical injury (22).

*Characterization of molecular heterogeneity among lupus glomeruli.* Although all lupus biopsies in this study were classified as WHO class III or WHO class IV and in all but two instances were obtained from patients with clinical renal disease with a duration of 1 month

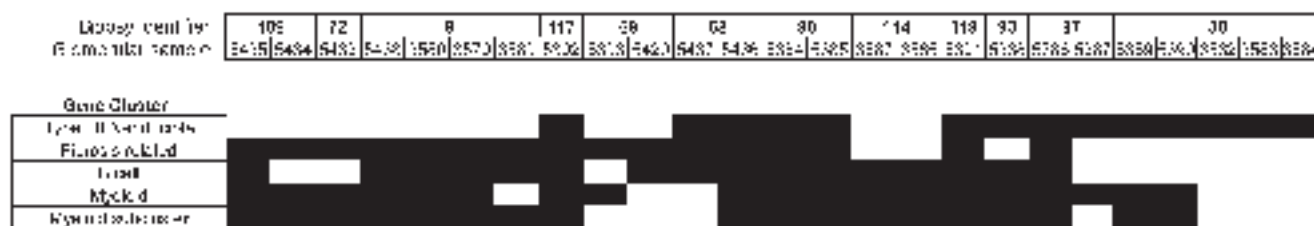


**Figure 5**  
Summary of expression pattern of gene clusters in each glomerular sample. Presence (shaded square) or absence (open square) of the expression of a gene cluster was determined by whether the average expression of the genes in each cluster or subcluster exceeded an increase of 1.5 fold relative to the average expression in the control glomeruli.

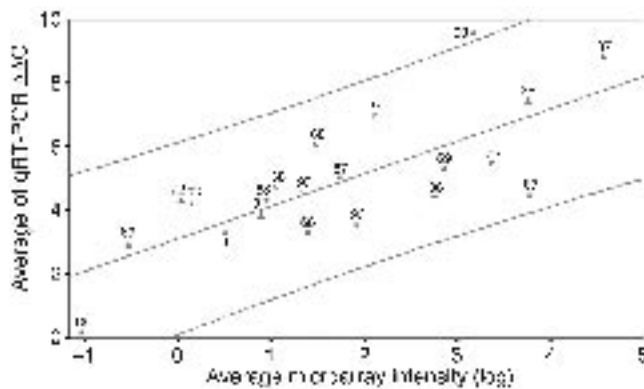


**Figure 6**  
This scatter plot depicts the linear regression line fit to the average expression of CTSC (squares), ISG15 (triangles), and MX1 (stars) determined by qRT-PCR or microarray analysis for each of the samples (indicated by the respective biopsy number) and each of the genes. The  $C_T$  cycle method was used to calculate the amplification of the genes by qRT-PCR relative to that of the reference control gene EEF1A1. The x axis is the mean of the logarithm of the intensities in the microarray experiment used for clustering for each of the tested genes in each sample. The two methods of analysis correlate significantly; the Spearman correlation coefficient is 0.754 ( $P = 0.0001$ ). The 95% confidence intervals of the regression line for individual data are shown.

or less (Table 2), they exhibited a distinct heterogeneity in gene expression, as illustrated in Figure 2B. Analysis of the variance in gene expression between biopsies, with grouping of all glomeruli from each biopsy, using a nested ANOVA algorithm (23) (data not illustrated) identified two main biopsy subgroups, designated SG1 and SG2. Hierarchical clustering of transcripts differentially expressed by these two subgroups demonstrated that biopsies in the SG1 group were characterized by strong expression of several genes in the fibrosis cluster, whereas the SG2 biopsies were distinguished by high expression of most of the transcripts previously identified as containing type I IFN response elements and low expression of the fibrosis-related genes that characterized SG1 biopsies (Figure 4).

Molecular heterogeneity was also examined at the level of the individual glomerulus. A scoring system was used to determine the presence or absence of a specific gene cluster to each glomerular sample (Figure 5). Transcripts with type I IFN response elements were concordantly expressed by all glomeruli in seven of twelve biopsies and were absent in all glomeruli in the remaining five samples. All but one glomerulus across all twelve biopsies were classified as expressing the cluster II (myeloid) transcripts; however, the expression level was variable, as seen in Figure 2B, and different glomeruli from the same biopsy were not always concordant in their expression of particular transcripts. The expression pattern of a myeloid subcluster that included CD14, FCER1G, IFI30, and CD163, among others (Supplemental Table 1), showed more heterogeneous distribution, being present in 18 of 25 glomeruli (Figure 5). Expression of the fibrosis cluster was assigned to 16 glomeruli (9 of 12 biopsies), with only one example (sample 87) of discordance between two glomeruli from the same biopsy. Expression of the B cell cluster was found in 16 glomeruli and partially overlapped expression of the fibrosis-related genes. Three of eight biopsies with two or more glomeruli diverged in expression of B cell genes.

*Validation of microarray expression by quantitative real-time PCR.* In order to determine whether the expression of transcripts obtained by the

microarray analysis could be independently validated by a method involving neither linear mRNA amplification nor microarray analysis, we performed quantitative real-time PCR (qRT-PCR) to independently quantify the relative abundance of mRNAs. For qRT-PCR, glomeruli were separately isolated by laser-capture microscopy. The RNA was extracted and converted to cDNA without prior amplification of RNA. Primers for CTSC, ISG15, and MX1 were selected because the expression of these transcripts differs significantly among samples (Figure 4), and the primers were used to amplify the respective cDNAs by qRT-PCR. For each renal sample, the level of expression of these transcripts was determined relative to the expression of a control transcript, eukaryotic elongation factor 1  $\alpha$ -1 (EEF1A1), amplified in a parallel qRT-PCR reaction. From each biopsy, four to nine replicates from one or more glomeruli were obtained and were analyzed separately by qRT-PCR. The linear regression line fit to the average expression of CTSC, ISG15, and MX1 determined by qRT-PCR or microarray analysis for each of the samples and each of the genes is shown in Figure 6 and illustrates that the two methods of analysis correlate significantly even though different glomeruli from the respective biopsies were used in each method; the Spearman correlation coefficient equals 0.754 ( $P = 0.0001$ ) in all samples studied.

*Relationship of molecular phenotype with histopathological studies.* Study of the relationship between the presence or absence of a specific gene cluster with the immunopathological findings of the biopsies revealed no overall correlation between activity and chronicity indices and gene expression (Table 3). However, there were a number of correlations with elements of the indices and individual gene clusters. All biopsies were also studied by immunohistochemistry using CD3 and CD68 staining (Table 1 and Figure 7), and these features of the biopsy were included in the correlations with individual gene clusters.

The expression of the genes with type I IFN response elements was associated with lower scores for three elements of the activity and chronicity indices: neutrophil infiltration, cellular crescents, and fibrous crescents. Moreover, these glomeruli were characterized by significantly smaller infiltration of CD3 T cells by histological scores. In contrast, renal biopsies containing glomeruli classified as expressing the fibrosis-related transcripts were distinguished by higher scores of the activity and chronicity indices, including cellular crescents, fibrous crescents, and wire loops. However, the presence of the fibrosis cluster was not uniformly associated with higher scores, as there was a trend toward decreased occurrence of necrosis. Interestingly, the expression of B cell genes by glomeruli paralleled the extent of histologic infiltration by CD3 T cells. It also

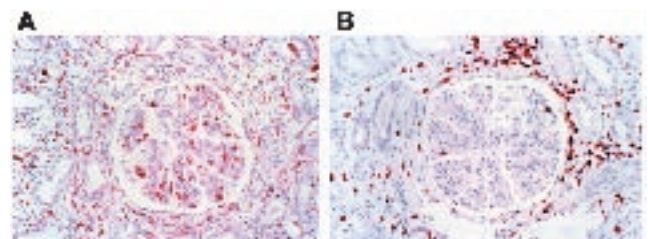


**Figure 7**  
Immunohistochemical staining of a lupus renal biopsy. (A and B) Monoclonal antibodies identifying CD68 (A) and CD3 (B) were used to stain lupus biopsies, followed by a second antibody and detection with peroxidase. Similar staining of control biopsies did not identify any reactive cells (data not shown). Magnification,  $\times 20$ .



correlated with the presence of cellular crescents, fibrous crescents, and interstitial inflammation. Table 3 additionally illustrates that while the total myeloid gene cluster was not significantly associated with any individual histopathological feature, the CD14-containing myeloid subcluster correlated with elements of the activity index, most notably endocapillary proliferation, wire loops, and cellular crescents, but not with necrosis. The expression of this subcluster also correlated with increased presence of CD68<sup>+</sup> cells by histological scores and a higher activity index. Differences in the clinical and laboratory features (Table 2) of the patients corresponding to the SG1 and SG2 subgroups of gene expression (Figure 4) did not account for these differences. In particular, the median duration of nephritis was the same in the two groups.

## Discussion

The combination of laser-capture isolation and microarray analysis allowed the use of “archival” renal biopsies to study molecular events involved in lupus glomerular disease and averted interference from distinct pathological events occurring in extraglomerular structures such as the renal interstitium and tubules. This work demonstrated that regularly processed clinical biopsies could be used if they were frozen within 1–2 hours of being obtained. Given the minute quantities of RNA obtained, linear amplification of RNA was an essential step for transcript quantification by microarray analysis. There is considerable support for the sensitivity and reproducibility of laser-capture microdissection and T7 promoter-based RNA amplification in the detection of transcription profiles even down to the single-cell level (24). In the present study, two lines of work supported the consistency of the results. First, the similarity of findings between two semi-independent data sets included in this analysis (Figure 2) allowed a degree of cross-validation showing that technical factors had minimal influence and supporting the choice to pool the two datasets for the main analysis. Second, the level of transcript expression for three informative genes was independently validated by qRT-PCR analysis using nonamplified RNA as the starting material, with analyses by the two methods correlating significantly (Figure 6).

A dominant feature of this study was the considerable degree of heterogeneity between lupus kidney biopsies in the increased expression of four main gene clusters, with each gene cluster reflecting the contribution of different pathways relevant to glomerular inflammation. These divergent features appear highly inconsistent with a unitary pattern of Arthus reaction-mediated necrosis and indicate that several different pathogenic elements are variably present in lupus nephritis. Interestingly, there was relatively less glomerulus-to-glomerulus molecular heterogeneity within a kidney than between kidneys, despite the variation in glomerular histopathological involvement within a kidney. We anticipate that the differences in these molecular patterns found in different kidneys will elucidate some of the marked heterogeneity in clinical outcome of lupus glomerulonephritis, but the design of this study did not allow this question to be addressed. However, the potential significance of each gene cluster to different pathological aspects of lupus nephritis was supported by the finding of associations of particular clusters with some elements of the activity and chronicity indices. No association was found, however, between transcriptional profiles and the WHO class III and IV subdivision of glomerulonephritis, indicating that similar molecular pathogenic processes characterize the two classes and that both exhibited equivalent heterogeneity in their transcriptional phenotype. A number of genes were consistently reduced

in expression across all glomeruli, including ion channels and transcription factors, suggesting a loss-of-function response to the glomerular inflammation.

The observed heterogeneity in gene expression among glomeruli in different biopsies (Figures 2 and 4) raises the important question of whether these differences identify subtypes of lupus nephritis or are a reflection of different stages in the progression of lupus nephritis. In support of the former possibility, both the SG1 and SG2 subgroups (Figure 4) had an equivalently high proportion of class IV proliferative nephritis, similar deposition of immune complexes and complement components, and in serum, similarly elevated antibodies to DNA and lowered complement levels (Table 2). The identical, relatively short mean duration of disease in both the SG1 and SG2 subgroups and comparable therapy in both groups prior to biopsy argues that the observed differences in transcriptional phenotype mainly reflect heterogeneity in the mechanisms of proliferative glomerulonephritis. However, serial gene expression profiles should be studied in consecutive renal biopsies to define more precisely the changes that occur in time. The trend toward mean higher serum creatinine levels in individuals with the SG1 classification of gene expression probably reflected a consequence of the processes occurring in the glomeruli.

The use of microarrays is a powerful tool for hypothesis generation that can lead to false-positive as well as false-negative conclusions, so it is imperative to cross-validate the present findings in a new study comprising a totally independent cohort of lupus glomeruli. It should be stressed, however, that the criteria used to select genes for clustering in this study were intentionally conservative, such as the requirement of a twofold change of expression in at least one third of lupus samples and control of the false discovery rate to less than 0.05. This resulted in the identification of fewer genes but at correspondingly greater levels of confidence.

The most widespread pattern of elevated gene expression in lupus glomeruli was for a large cluster of transcripts identified as being expressed mainly by cells of the myeloid lineage. We attempted to identify the particular myeloid lineages present in the glomerulus by using a peripheral blood reference panel and obtained evidence that was compatible with the presence of activated monocytes/macrophages, activated dendritic cells, and activated neutrophils (Figure 3). However, it was not possible to clearly distinguish the lineages present in the glomeruli due to the large number of genes with overlapping expression among the various myeloid cell types. These findings emphasize the importance and the complexity of the myeloid lineages found in the nephritic kidney and they are consistent with observations in the NZB/W mouse model of spontaneous lupus-like nephritis (3, 25).

The myeloid subcluster that included CD14 exhibited more variation in glomerular expression than the myeloid cluster and correlated with certain features within the activity index, including cellular crescents, endocapillary proliferation, and wire loops, but not with others, such as necrosis (Table 3), which suggests that a particular subset or activation pattern of macrophages accounts for certain features present in active lupus nephritis. The transcriptional signature of the myeloid subcluster also correlated with immunohistochemical staining by CD68, providing an additional cross-validation of the microarray results. These findings are consistent with the proposed inclusion of increased macrophage numbers in a modified activity index proposed by Hill et al. (7) and emphasize the importance of this lineage in lupus glomerulonephritis.



Signaling through the activating FcR $\gamma$ c chain is central to the immune complex-mediated glomerular injury that occurs in the NZB/W mouse model of lupus nephritis (3). It was therefore especially interesting to find an increase in the expression of FcR $\gamma$ c in the CD14 myeloid subcluster, suggesting that a similar pathway of macrophage activation may occur in the human disease. Expression of the “classic” FcRs that signal through FcR $\gamma$ c has been difficult to demonstrate in the glomerulus and is an area of investigation (26). In this context, it is intriguing to find increased expression of FCGBP (Fc $\gamma$ -binding protein), an FcR previously unknown in the kidney and previously identified only on placenta and colonic epithelium (27). The increased glomerular expression of other cell surface receptors such as CD36 and CD163 suggests additional pathways that may be involved in the handling of glomerular immune complexes.

T cells infiltrate the kidney in lupus nephritis (28), and small numbers were clearly identified in most glomeruli by immunohistochemistry (Table 1 and Figure 7B); however, relatively few T cell lineage genes were identified by microarray analysis. This low number may reflect the strict selection criteria used for clustering analysis and may be a false-negative finding. However, the increased expression of transcripts in the pathway of MHC class II antigen presentation suggests a glomerular potential to present peptide (auto-) antigens to T cells. The presence in the glomerulus of a small cluster of genes characterizing B cells and plasma cells correlated with numbers of glomerular T cells, and in turn with high scores for interstitial inflammation and crescents (Table 3) suggests that these lymphocytes are present in concert with these processes, as has been observed in the NZB/W mouse during nephritis (25). This raised the possibility that cognate T cell-B cell interaction possibly driven by autoantigen recognition occurs in the kidney and could enhance both glomerular injury and the autoimmune response. The finding of increased expression of the IFN- $\gamma$ -induced IFI30 and of Eta-1 in lupus glomeruli together with decreased expression of TGF- $\beta$  point to an environment that would favor Th1 cell differentiation. Eta-1 has been associated with the development of Th1-mediated immunity (29). IFN- $\gamma$  has been identified as a major effector molecule that drives the development of lupus in murine models of the disease (30). While the role of the T cell in the nephritic glomerulus remains incompletely documented in these microarray experiments, it was interesting to find a relative accumulation of CD3<sup>+</sup> cells in periglomerular interstitial regions of the lupus biopsies that were studied by microarray (Figure 7B), raising the separate question of why T cells preferentially accumulate in the interstitium.

Global glomerulosclerosis or fibrosis characterizes end-stage renal disease regardless of specific etiology, and a clinically important issue in lupus nephritis is to identify the individuals who will probably progress to renal fibrosis. The observation that in different biopsies the expression of the fibrosis cluster correlated with the presence of crescents and the hyaline matrix deposition of wire loops (Table 3) suggests that these transcripts indeed mediate certain elements of glomerulosclerosis. Interestingly, although there was one instance of divergent glomerulus-to-glomerulus expression of the fibrosis genes, in most biopsies, the pattern of fibrotic gene expression was usually found in both glomeruli with morphological evidence of sclerosis and glomeruli with minimal or no involvement at the morphological level. This suggests that the early identification of this pattern in glomeruli with little histopathological evidence of frank glomerulosclerosis or crescent formation may denote an individual at high risk of progression to this response.

Transcripts for collagen I  $\alpha$ 2 and collagen VI  $\alpha$ 3 are increased in lupus glomeruli as part of the fibrosis cluster. Both transcripts are also increased in diabetic glomerulosclerosis and crescentic glomerulonephritis through a pathway involving TGF- $\beta$ 1 (16, 20, 25). Intriguingly, in terms of the mechanism of fibrosis in lupus, the present study suggests it does not occur through a TGF- $\beta$ 1-mediated pathway, as lupus glomeruli exhibit a striking decrease in expression of TGF- $\beta$ 1 and two of its receptor proteins, as well as the TGF- $\beta$ 1-induced PAI-1 (15). Conversely, there are several genes that could play a role in regulating the development of lupus glomerulosclerosis: MCP-1 is highly expressed in the fibrosis-related cluster and has previously been linked to some forms of nephropathy (21), and the increase in matrilysin (MMP7) is significant, as MMP7 promotes fibrosis in interstitial pneumonitis (31).

Another member of the fibrosis cluster is RUNX1, encoding a hematopoietic transcription factor that is emerging as a central transcriptional regulator in autoimmune disease. The RUNX1 product interacts with PDCD1, located at chromosome 2q37 and encoding a transcript that regulates programmed cell death. PDCD1 has been identified as a strong candidate gene for increasing susceptibility to SLE (32) through a single-nucleotide polymorphism that alters a RUNX1 binding site. Recently, susceptibility to rheumatoid arthritis (33) and to psoriasis (34) were also shown to be associated with genes that contained altered binding sites for RUNX1 and that were encoded by loci located at chromosomes 5q31 and 17q25, respectively.

One of the more striking features of lupus glomeruli was the pattern of high expression of genes with promoters containing type I IFN response elements that was found in approximately half of the biopsies and accounted for most of the genes in the SG2 subgroup. The expression of these transcripts was highly concordant among all glomeruli from the same biopsy, suggesting that an extraglomerular process may regulate their presence in the kidney. Although the expression of genes with type I IFN response elements in lupus glomeruli could be responsible for glomerular injury in the SG2 group, their presence in these glomeruli was inversely correlated with that of many genes in the fibrosis cluster and with the presence of cellular and fibrous crescents, otherwise considered as histological elements indicating a “high-risk” of lupus nephritis (35). This suggests that an event related to the expression of these transcripts might either cause a milder form of renal injury or be a protective response to glomerular injury. If protective, however, the presence of fibrosis-related transcripts in a few of the SG2 glomeruli emphasizes that the protection from glomerulosclerosis is not absolute.

In terms of the mechanism responsible for the coordinate induction of the genes containing type I IFN response elements in glomeruli, there was no evidence of elevated glomerular levels of IFN- $\alpha$  transcripts, although IFN- $\alpha$  is elevated in peripheral blood of some individuals with SLE (36, 37). Moreover, preliminary data demonstrate that the increased expression of type I IFN-inducible transcripts by the SG2 group of lupus biopsies (Figure 4) is restricted to the glomerulus, as qRT-PCR analyses of ISG15 and MX1 in renal interstitial tissue was markedly lower than in the corresponding glomerulus (data not shown). This also emphasizes the technical importance of studying gene expression in individual renal compartments.

Recently it was demonstrated that type I IFN-inducible transcripts are increased in peripheral blood leukocytes of some individuals with active lupus (38, 39), and it is possible that this elevation could parallel the glomerular increase in type I IFN-inducible transcripts observed in this study. The present finding that activated NK cells



express all of the type I IFN response element-containing transcripts that were identified in lupus glomeruli suggests one additional interpretation of this “signature” in the kidney: that the entrance of activated NK cells could be responsible for this phenotype, mediating either an injurious or a protective effect. This is supported by the finding that a few genes not containing type I IFN response elements were also included in this cluster and were increased in NK cells.

Perhaps also related to this is the observation that some type I IFN-inducible transcripts identified in this study were located in genomic regions associated with the lupus susceptibility. *MNDA* is found in the lupus susceptibility region at 1q22 (40), and *ifi202*, a murine homolog of *MNDA* that is encoded by a region syntenic to 1q22, is an interesting gene indicating susceptibility to lupus in the mouse (41). A second IFN-inducible gene, *SP100*, is located within another region associated with lupus susceptibility in the human genome, at 2q36-37 (40). This aspect of the action of some type I IFN-inducible transcripts may be relevant to the development of autoimmune phenomena that occasionally appear during the use of IFN- $\alpha$  in the treatment of chronic viral hepatitis and certain malignancies (42). However, until the significance of the expression of type I IFN-inducible genes in lupus is better understood, some caution may be warranted if considering blockade of IFN- $\alpha$  induction as a therapeutic target.

## Methods

**Clinical samples.** The biopsies were from individuals with SLE who had newly identified renal involvement leading to diagnostic renal biopsy and for which there was abundant residual “archival” frozen tissue (Table 2). Controls were kidney biopsies that appeared normal by histopathological examination. These were either from kidneys in which there was minimal isolated proteinuria or hematuria but no pathological abnormalities were identified by renal biopsy, or from uninvolved portions of a kidney at the time of nephrectomy for tumor. One study population (called B13) included 11 individuals with lupus nephritis (17 independently processed glomeruli) and 2 control individuals (3 independently processed glomeruli). A second sample set (called B12) included eight glomeruli isolated from three SLE biopsies and three control glomeruli from two different control individuals. Some SLE biopsies, represented by different glomeruli, were studied in both sample sets. The two sample sets were processed at different times and were analyzed on slightly different versions of the cDNA microarray, as indicated in Methods, *cDNA microarray*. All biopsies had been stored at  $-80^{\circ}\text{C}$  from several months to more than a year before being processed for microarray analyses, and only those biopsies that had been frozen within approximately 1 hour of collection were used for laser capture. Standard histological, immunofluorescence, and electron microscopy studies were used to classify the biopsies (Table 1) (4, 6). Quantification of infiltrating T cells (CD3) and macrophages (CD68) was done using immunoperoxidase staining of formalin-fixed tissue. For gene expression analyses, if more than one glomerulus was analyzed from the biopsy, each glomerulus was isolated by laser-capture microscopy, processed, and analyzed individually by microarray hybridization. The use of “archival” renal biopsies and clinical data reported in this study were approved by the Columbia University Institutional Review Board (IRB 0144).

**Laser-capture microscopy and RNA/cDNA sample preparation.** For each glomerular sample, four to six sections 7  $\mu\text{m}$  in thickness of a frozen biopsy were used for laser capture of consecutive levels of the same glomerulus (10, 43) to minimize sampling effect within

a glomerulus. Approximately 1–5 ng of RNA were extracted from each laser-captured glomerular sample. After two rounds of T7 promoter-based RNA amplification, each sample typically provided a final yield of 50–100  $\mu\text{g}$  of amplified mRNA (10, 24). Because of the potential for transcript truncation or degradation, no sample was processed further unless the adequacy of each amplification was verified by quantitative PCR amplification of aliquots of RNA removed prior to and after each step in the amplification process using primers specific for proximal and distal exons of a ubiquitous eukaryotic elongation factor (EEF1A1) as described (24). The overall quality of the amplified RNA was also assessed by agarose gel electrophoresis (data not shown).

**cDNA microarray.** The human cDNA microarrays were spotted onto Corning GAPS slides (Corning Life Sciences, Acton, Massachusetts, USA) using an Amersham Biosciences Generation III spotter (Amersham Biosciences, Piscataway, New Jersey, USA). The B12 array contained 3,602 genes and the B13 array had the same 3,602 genes plus an additional 428 genes. Each clone was spotted in duplicate on the array. Of the clones on the array, 59% were IMAGE clones purchased from Research Genetics (Invitrogen, Carlsbad, California, USA). The microarrays contained a set of expressed human genes that were chosen based on the availability of human cDNA clones at that time rather than their functional characteristics. The major functional families of cDNAs on the microarray included receptor molecules (25% of clones), ion channels (6.5% of clones), immunoglobulin family (1% of clones), cytokines and chemokines (3.3% of clones), enzymes (18% of clones), adhesion molecules (4% of clones), transporters (5% of clones), signal transduction molecules (5% of clones), DNA-binding molecules (2.6% of clones), and chaperones (3.2% of clones). The indocarbocyanine-labeled cDNA probe preparation, hybridization, and subsequent washes of the arrays were performed according to the methods described by Luo et al. (10). The arrays were scanned in a ScanArray 4000 (Perkin Elmer Life Sciences, Boston, Massachusetts, USA). Quantification was done using Imagene (Biodiscovery, Marina del Rey, California, USA).

**Quantitative PCR analysis.** Total RNA was extracted from two to four laser-captured glomeruli isolated as described above using the Qiagen Micro RNA kit (Qiagen Inc., Valencia, California, USA). Total RNA was converted to cDNA without prior amplification of RNA using the First Strand Synthesis System (Invitrogen) and an oligodT primer.

The cDNA (0.4  $\mu\text{l}$  for each reaction) was subjected to SYBR green-based qRT-PCR using a Smart Cycler (Cepheid, Sunnyvale, California, USA) according to the manufacturer’s instructions. The target *CTSC*, *ISG15*, and *MX1* genes were amplified using the following primers: for *CTSC*, CAGACCCAATCCTAAGCCCTCAG (5′) and GCCATAGCCCACAAGCAGAACAGC (3′); for *ISG15*, GGCGGGCAACGAATTCAGGTGT (5′) and CTCCCCGAGCGCGCAGATTCA (3′); and for *MX1*, TGCTGCATCCCACCCCTCTATTACT (5′) and GCGGATGGCATTCTGGGCTTTAT (3′). Amplification of the reference gene *EEF1A1* using primers CATGCAAGTTTGCTGAGCTG (5′) and GATGCATTGTTATCATTAACC (3′) and of a negative control was included in each experiment in separate reactions. Because the quantity of the template was limited, DNase treatment was not performed and instead the two primers were designed so that the target cDNA spanned at least one intron in the genomic sequence. The qRT-PCR reaction was performed in the presence of 20 mM Tris-HCl, pH 8.4, 50 mM KCl, 3 mM MgCl<sub>2</sub>, 0.2% Tween-20, 0.15 M Trehalose, 0.2 mg/ml BSA,



0.4 mM dNTPs, 0.4× SYBR green, 0.1 U Platinum Taq Polymerase (Invitrogen), and 12.5 pmol of each primer per reaction in total reaction volume of 25  $\mu$ l. The quantity of input cDNA was titrated to determine the concentration range at which the efficiencies of target and reference were approximately equivalent. The specificity of the resulting amplifications were confirmed by a melting curve in each experiment, and experiments were considered valid only if the melting curve showed a single peak at the expected melting temperature for each PCR product. The comparative threshold ( $C_T$ ) cycle method was used to calculate the amplification of the genes relative to the reference control gene EEF1A1. Because the microarray clustering analyses were performed using the normalized value of the logarithm of the intensity, the analysis of the kinetic PCR quantification was made using  $\Delta C_T$  values rather than “fold changes,” which would involve exponentiation. The  $\Delta\Delta C_T$  value for each data point was calculated by using the negative of the value obtained by first subtracting the  $C_T$  for the reference gene from the target and then subtracting the  $\Delta C_T$  calibrator value, or  $\Delta\Delta C_T = -[(C_{T \text{ target}} - C_{T \text{ reference}}) - C_{T \text{ target calibrator}}]$ , where  $C_{T \text{ target calibrator}}$  was the numerically greatest observed  $C_T$  value for a given target across all experiments. Four to nine replicates were determined for each sample. The correlation between the means of the determinations for each target by the  $C_T$  cycle method versus the mean logarithm of the intensities in the microarray experiment for the same target was assessed by calculation of the nonparametric Spearman rho coefficient, and the linear regression of the scatter plot was calculated using SPSS (SPSS, Chicago, Illinois, USA).

**Microarray data normalization.** The cDNA synthesized from each control or SLE glomerular RNA sample was hybridized to two microarray slides that each contained a cDNA array spotted in duplicate, yielding a quadruplicate data set for each sample. Outliers were automatically excluded prior to normalization (44). For analysis, the intensities from each data set were scaled at the 75th percentile (the 75th percentile value of each data set was set to 100) followed by log transformation in base 2, and then were normalized in a two-step procedure (44). The first normalization step was performed across arrays within the same RNA sample. The mean intensity of the quadruplicates was then determined, yielding a matrix of the expression values for 4,030 genes and 31 samples (25 SLE glomeruli and 6 control glomeruli). A second normalization was performed across control and SLE samples within each of the two experimental sets, B12 and B13. The resulting, unanalyzed data file is in Supplemental Table 2, which is subdivided according to the two data sets.

**Microarray analyses of a peripheral blood reference panel.** A reference set of cells was isolated from the peripheral blood of one to five normal donors, depending on the cell type. Monocytes, NK cells, B cells, and T cells were isolated from Ficoll Hypaque-purified PBMC samples using CD14-, CD56-, CD19- and CD4/CD8-coupled Miltenyi beads, respectively (Miltenyi Biotec, Cologne, Germany). Basophils were isolated from PBMC samples using the Miltenyi Basophil Isolation Kit 4. Neutrophils and eosinophils were isolated from non-PBMC samples using CD16- and CD15-coupled Miltenyi beads, respectively. Activated CD14 cells or neutrophils were stimulated in overnight cultures in the presence of LPS or PMA, as indicated in Figure 3. Immature dendritic cells were obtained after a 7-day culture of CD14 cells in the presence of IL-4 and GM-CSF, and dendritic cells were isolated after an additional 24-hour incubation in the presence of TNF- $\alpha$ . Activated NK cells were obtained after an overnight culture of CD56

cells in the presence of LPS. Activated B cells were prepared by incubation of CD19 cells overnight in CD40-coated wells or in the presence of PMA. CD4 T cells and CD8 T cells were activated by overnight culture in the presence of OKT3 (mouse monoclonal antibody to human CD3) and CD28. RNA extraction, cDNA probe preparation, and cDNA microarray hybridization were done as described below, with the exception that RNA was not amplified prior to cDNA synthesis.

**Selection of genes that differ in expression between SLE glomeruli and controls.** Transcripts unlikely to contribute significantly to the differential gene expression profiles of the two groups of glomeruli were filtered out first by determination of the difference in gene expression between lupus glomeruli and controls on the final normalized data for each gene on the microarray using a Welch modified *t* test (S-PLUS 2000; Insightful, Seattle, Washington, USA). A Benjamini and Hochberg (45) stepwise procedure was used to control the false discovery rate below 0.05. Genes with adjusted *P* values greater than 0.05 were considered not to have significant differences between SLE and controls and were removed from further analysis.

The second selection step was based on calculation of the log ratio of expression between experiment and control for each gene, using for the control value the expression of the gene averaged across all controls (C-avg.). As the expression values were already “log transformed,” this ratio was obtained by subtraction of C-avg. from the log expression value of the gene in each sample. In this selection step, we included only genes that had a change in this log ratio of at least a twofold in one third or more of the SLE glomeruli, resulting in 177 genes that were selected for subsequent cluster analysis.

**Cluster analysis.** The log ratios for the expression of each of the 177 genes, as defined above, were clustered in the OmniViz version 3.0 software (OmniViz Inc.). An agglomerative hierarchical cluster analysis was performed using average linkage and a correlation metric unless otherwise stated.

**Subgrouping of SLE samples and selection of subgroup-specific genes.** The variance of each gene among the 11 different SLE biopsies in set B13 was estimated individually by a nested ANOVA model (S-PLUS 2000; Insightful); the structure of the data was biopsy/glomerular sample. Using this model, genes with high biopsy-to-biopsy variance were selected ( $P \leq 0.05$ ) and the ratio of the expression in each SLE glomerulus to the mean expression in the controls was calculated for each gene and was analyzed by hierarchical clustering. This identified the two biopsy subgroups designated SG1 and SG2.

Differential gene expression between SG1 and SG2 was then determined for each gene by nested ANOVA using the structure SLE subgroup/biopsy/glomerular sample. The Benjamini and Hochberg procedure was further applied to keep the false discovery rate below 0.05 (45). Genes were selected based on adjusted *P* values of 0.05 or less and a ratio of twofold or more between the mean of the expression in SG1 versus SG2. For the selected genes, the ratio of their expression in each SLE glomerulus over the mean of the controls was analyzed by hierarchical clustering using average linkage and a Euclidean correlation metric.

**Expression of individual gene clusters in each glomerular sample and the correlation to histopathological markers of disease.** To obtain an overall measure of the expression of a gene cluster by individual glomeruli, we calculated the mean value of the intensity scores (log ratio of expression in a lupus sample over geometric mean of controls) for all genes in the cluster. A value of 0.6 or more (equal to a change of approximately 1.5-fold over controls) was used to indicate expression of a cluster by a glomerular sample. The semiquantitative



morphological variables (immunopathology and markers of activity and chronicity) characterizing each glomerular sample were then compared between the group of glomeruli expressing a certain gene cluster and the group not expressing the gene cluster using the Wilcoxon rank sum test in SPSS.

### Acknowledgments

Ann Moriarty, Didier Leturcq, and Juli DeGraw (Johnson & Johnson Pharmaceutical Research and Development) are gratefully acknowledged for allowing us to use data from their unpublished microarray analyses of a set of peripheral blood cell cultures. We also thank Valeria Steshenko for performing the qRT-PCR analyses; Lin Luo and Anton Bittner for excellent technical assistance; and Fredrik Kamme and Xiao-Jun Ma for valuable discussions.

This study was in part supported by grants from the National Institutes of Health (P30 HD34611, K01 DK002853, U19 AI046132, and K12 HD43389).

Received for publication June 6, 2003, and accepted in revised form April 9, 2004.

Address correspondence to: Karin S. Peterson, Department of Pediatrics, Columbia University, PH4-477, 630 168th Street, New York, New York 10032, USA. Phone: (212) 305-5766; Fax: (212) 305-9078; E-mail: ksp4@columbia.edu.

Mark Erlander's present address is: Arcturus Applied Genomics, Carlsbad, California, USA.

- Kotzin, B.L. 1996. Systemic lupus erythematosus. *Cell*. **85**:303–306.
- Peterson, K., and Winchester, R. 2001. Systemic lupus erythematosus: pathogenesis. In *Arthritis and allied conditions, a textbook of rheumatology*. W. Koopman, editor. Lippincott, Williams and Wilkins. Baltimore, Maryland, USA. 1503–1532.
- Clynes, R., Dumitru, C., and Ravetch, J.V. 1998. Uncoupling of immune complex formation and kidney damage in autoimmune glomerulonephritis. *Science*. **279**:1052–1054.
- D'Agati, V. 1998. Renal disease in systemic lupus erythematosus, mixed connective tissue disease, Sjogren's syndrome and rheumatoid arthritis. In *Heptinstall's pathology of the kidney*. J.C. Jennette, J.L. Olson, M.M. Schwartz, and F.B. Silva, editors. Lippincott-Raven. Philadelphia, Pennsylvania, USA. 541–624.
- Pollak, V.E., and Pirani, C.L. 1969. Renal histologic findings in systemic lupus erythematosus. *Mayo Clin. Proc.* **44**:630–644.
- Austin, H.A., 3rd, Muenz, L.R., Joyce, K.M., Antonovych, T.T., and Balow, J.E. 1984. Diffuse proliferative lupus nephritis: identification of specific pathologic features affecting renal outcome. *Kidney Int.* **25**:689–695.
- Hill, G.S., et al. 2000. A new morphologic index for the evaluation of renal biopsies in lupus nephritis. *Kidney Int.* **58**:1160–1173.
- Alizadeh, A.A., et al. 2000. Distinct types of diffuse large B-cell lymphoma identified by gene expression profiling. *Nature*. **403**:503–511.
- Higgins, J.P., et al. 2004. Gene expression in the normal adult human kidney assessed by complementary DNA microarray. *Mol. Biol. Cell* **15**:649–656.
- Luo, L., et al. 1999. Gene expression profiles of laser-captured adjacent neuronal subtypes. *Nat. Med.* **5**:117–122.
- Yim, S.H., et al. 2003. Microarray analysis using amplified mRNA from laser capture microdissection of microscopic hepatocellular precancerous lesions and frozen hepatocellular carcinomas reveals unique and consistent gene expression profiles. *Toxicol. Pathol.* **31**:295–303.
- Luzzi, V., Mahadevappa, M., Raja, R., Warrington, J.A., and Watson, M.A. 2003. Accurate and reproducible gene expression profiles from laser capture microdissection, transcript amplification, and high density oligonucleotide microarray analysis. *J. Mol. Diagn.* **5**:9–14.
- Matsui, H., et al. 2003. Gene expression profiles of human BPH (II): Optimization of laser-capture microdissection and utilization of cDNA microarray. *Anticancer Res.* **23**:195–200.
- National Center for Biotechnology Information. <http://www.ncbi.nlm.nih.gov/LocusLink>.
- Rerolle, J.P., Hertig, A., Nguyen, G., Sraer, J.D., and Rondeau, E.P. 2000. Plasminogen activator inhibitor type 1 is a potential target in renal fibrogenesis. *Kidney Int.* **58**:1841–1850.
- Wolf, G., and Ziyadeh, F.N. 1999. Molecular mechanisms of diabetic renal hypertrophy. *Kidney Int.* **56**:393–405.
- O'Farrell, C., et al. 2002. Survey of transcript expression in rainbow trout leukocytes reveals a major contribution of interferon-responsive genes in the early response to a rhabdovirus infection. *J. Virol.* **76**:8040–8049.
- Urban, B.C., Willcox, N., and Roberts, D.J. 2001. A role for CD36 in the regulation of dendritic cell function. *Proc. Natl. Acad. Sci. U. S. A.* **98**:8750–8755.
- Suzuki, T., et al. 2000. Differential involvement of Src family kinases in Fc gamma receptor-mediated phagocytosis. *J. Immunol.* **165**:473–482.
- Maric, M., et al. 2001. Defective antigen processing in GILT-free mice. *Science*. **294**:1361–1365.
- Lloyd, C.M., et al. 1997. RANTES and monocyte chemoattractant protein-1 (MCP-1) play an important role in the inflammatory phase of crescentic nephritis, but only MCP-1 is involved in crescent formation and interstitial fibrosis. *J. Exp. Med.* **185**:1371–1380.
- Hilgers, K.F., et al. 2000. Monocyte chemoattractant protein-1 and macrophage infiltration in hypertensive kidney injury. *Kidney Int.* **58**:2408–2419.
- Kerr, M.K., Martin, M., and Churchill, G.A. 2000. Analysis of variance for gene expression microarray data. *J. Comput. Biol.* **7**:819–837.
- Kamme, F., et al. 2003. Single-Cell microarray analysis in hippocampus CA1: demonstration and validation of cellular heterogeneity. *J. Neurosci.* **23**:3607–3615.
- Schiffer, L., et al. 2003. Short term administration of costimulatory blockade and cyclophosphamide induces remission of systemic lupus erythematosus nephritis in NZB/W F1 mice by a mechanism downstream of renal immune complex deposition. *J. Immunol.* **171**:489–497.
- Uciechowski, P., et al. 1998. IFN-gamma induces the high-affinity Fc receptor I for IgG (CD64) on human glomerular mesangial cells. *Eur. J. Immunol.* **28**:2928–2935.
- Harada, N., et al. 1997. Human IgGFc binding protein (FcgammaBP) in colonic epithelial cells exhibits mucin-like structure. *J. Biol. Chem.* **272**:15232–15241.
- Yellin, M.J., et al. 1997. Immunohistologic analysis of renal CD40 and CD40L expression in lupus nephritis and other glomerulonephritides. *Arthritis Rheum.* **40**:124–134.
- Jansson, M., Panoutsakopoulou, V., Baker, J., Klein, L., and Cantor, H. 2002. Cutting edge: Attenuated experimental autoimmune encephalomyelitis in eta-1/osteopontin-deficient mice. *J. Immunol.* **168**:2096–2099.
- Theofilopoulos, A.N., Koundouris, S., Kono, D.H., and Lawson, B.R. 2001. The role of IFN-gamma in systemic lupus erythematosus: a challenge to the Th1/Th2 paradigm in autoimmunity. *Arthritis Res.* **3**:136–141.
- Zuo, F., et al. 2002. Gene expression analysis reveals matrix metalloproteinase-1 as a key regulator of pulmonary fibrosis in mice and humans. *Proc. Natl. Acad. Sci. U. S. A.* **99**:6292–6297.
- Prokunina, L., et al. 2002. A regulatory polymorphism in PDCD1 is associated with susceptibility to systemic lupus erythematosus in humans. *Nat. Genet.* **32**:666–669.
- Tokuhiro, S., et al. 2003. An intronic SNP in a RUNX1 binding site of SLC22A4, encoding an organic cation transporter, is associated with rheumatoid arthritis. *Nat. Genet.* **35**:341–348.
- Helms, C., et al. 2003. A putative RUNX1 binding site variant between SLC9A3R1 and NAT9 is associated with susceptibility to psoriasis. *Nat. Genet.* **35**:349–356.
- Austin, H.A., 3rd, Boumpas, D.T., Vaughan, E.M., and Balow, J.E. 1995. High-risk features of lupus nephritis: importance of race and clinical and histological factors in 166 patients. *Nephrol. Dial. Transplant.* **10**:1620–1628.
- Hooks, J.J., et al. 1979. Immune interferon in the circulation of patients with autoimmune disease. *N. Engl. J. Med.* **301**:5–8.
- Bengtsson, A.A., et al. 2000. Activation of type I interferon system in systemic lupus erythematosus correlates with disease activity but not with antiretroviral antibodies. *Lupus*. **9**:664–671.
- Baechler, E.C., et al. 2003. Interferon-inducible gene expression signature in peripheral blood cells of patients with severe lupus. *Proc. Natl. Acad. Sci. U. S. A.* **100**:2610–2615.
- Bennett, L., et al. 2003. Interferon and granulopoiesis signatures in systemic lupus erythematosus blood. *J. Exp. Med.* **197**:711–723.
- Wakeland, E.K., Liu, K., Graham, R.R., and Behrens, T.W. 2001. Delineating the genetic basis of systemic lupus erythematosus. *Immunity*. **15**:397–408.
- Rozzo, S.J., et al. 2001. Evidence for an interferon-inducible gene, Ifi202, in the susceptibility to systemic lupus. *Immunity*. **15**:435–443.
- Stegmann, J.L., et al. 2003. High incidence of autoimmune alterations in chronic myeloid leukemia patients treated with interferon-alpha. *Am. J. Hematol.* **72**:170–176.
- Marras, D., et al. 2002. Replication and compartmentalization of HIV-1 in kidney epithelium of patients with HIV-associated nephropathy. *Nat. Med.* **8**:522–526.
- Shaw, K.J., et al. 2003. Comparison of the changes in global gene expression of *Escherichia coli* induced by four bactericidal agents. *J. Mol. Microbiol. Biotechnol.* **5**:105–122.
- Benjamini, Y., and Hochberg, Y. 1995. Controlling the false discovery rate: a practical and powerful approach to multiple testing. *J. Royal Stat. Soc. Ser. B.* **57**:289–300.